Microfluidic cell sorter for use in developing red fluorescent proteins with improved photostability: Supplemental Material

Lloyd M. Davis,[a] Jennifer L. Lubbeck,[bc] Kevin M. Dean,[b] Amy E. Palmer[bd] and Ralph Jimenez[bc]

[a] Visiting Fellow at JILA; Permanent address: Department of Physics, University of Tennessee Knoxville, and Center for Laser Applications, University of Tennessee Space Institute, 411 B.H. Goethert Parkway, Tullahoma, Tennessee 37388, USA. E-mail: ldavis@utsi.edu
[b] Department of Chemistry & Biochemistry, University of Colorado Boulder, 215 UCB, Boulder, Colorado 80309, USA. E-mails: jennifer.lubbeck@colorado.edu, kevin.dean@colorado.edu
[c] JILA, University of Colorado Boulder, 440 UCB, Boulder, Colorado 80309, USA. E-mail: rjimenez@jila.colorado.edu
[d] BioFrontiers Institute, University of Colorado Boulder, 596 UCB, Boulder, Colorado 80309, USA. E-mail: amy.palmer@colorado.edu

Software for real-time analysis of fluorescence peaks and control of cell sorter: Target PC program

Table 1 gives a flow diagram of the main parts of the algorithm of the Target PC program, which finds peaks, counts them into bursts, and categorizes and counts bursts of different types based on the values of adjustable parameters (which are Underlined). In the main loop, at line 9 the program awaits a block of data (typically 625 points in 5 ms), then at line 10 it finds the locations and amplitudes of peaks in the data stream using the LabView library routine *Peak Detector*, which is a point-by-point routine that retains needed data from prior calls. This finds peaks above an adjustable level (set at the current average plus an adjustable Threshold so as to recognize a wide dynamic range but yet distinguish partially overlapping peaks) by fitting a quadratic of given Width to the data stream (so that peaks of small width due to noise are not found). In the for-loop of lines 11–37, the timings of peaks are used to count up peaks into bursts. The count, i, is reset to the beginning value (i = 0;) designating the first peak of a burst whenever the time since the last peak is not within the set limits (between Min and Max at lines 17 or 24, or for the monitor between $(1-\delta) \, T_D$ and $(1+\delta) \, T_D$ at line 33), or whenever the count equals the number of laser beams used (at lines 27 or 36). If this first peak follows the previous peak too closely, the burst that follows will be flagged as overlapping (line 40 or 41). An array (A[ ]) is used to store the amplitude of the first peak and the normalized amplitudes of subsequent peaks in a burst. After a cell has passed through all photobleaching laser beams, if all the amplitudes are between the lower limits and upper limits (which are defined in the arrays LL[ ] and UL[ ], i.e., LL[j]<A[j]<UL[j] for j=0,1, …, N) and the burst is not overlapping with a prior one (O=false at line 21), the time and speed for the motion of the 1064-nm laser spot is calculated (line 22, Calculate timing) using the procedure discussed in the text in the section **Timing set-up**, taking into account the positions of the peaks in the data stream and the amount of time that has elapsed during the computation, as determined from readings of the Target PC clock. If the piezo-tilt mirror has completed its previous trajectory and if there is sufficient time to intercept the cell, a subprogram (line 22, Initiate selection), which will send the calculated voltages from the DAQ card with the calculated timing, is started; at this time the flag for 'Selected' is set true.

After the peaks are counted for a cell passing through all photobleaching beams, the next peak will be reset to the beginning of a new burst if the monitor beam is not used (line 27) or will be tested to see if it corresponds to a monitor peak (line 30), in which case the next peak will be reset to the beginning of a new burst (line 36). With completion of a burst in either of the two cases of these possible resets after all photobleaching beams are counted, the type of the burst is determined and a counter for the particular burst type is incremented. Note that (in line 21) a burst may be selected only if it does not overlap with the prior burst. However, whether selected or not, it will be designated as overlapping if it overlaps with either the prior or the following burst (lines 27, 28 or 33, 34, or 36, 37).

Table 1 Flow diagram of Target algorithm:

1   $\underline{N}$ = 2, 3, 4, 5, 6, 7, or 8 = number of photobleaching beams used
2   $\underline{M}$ = 0, or 1 = if monitor beam is blocked, or used
3   i = $\underline{N}$ + $\underline{M}$; // initialize count of peaks in the present burst (to cause the call of subroutine Reset on initialization)
4   S = false;   // initialize flag S to indicate if the burst is selected
5   O = false;   // initialize flag O to indicate if the burst overlaps with the prior one
6   sou = 0; nou = 0; som = 0; nom = 0; sgu = 0; ngu = 0; sgm = 0; ngm = 0;
7   // initialize counters of bursts, s/n = selected/not selected, o/g = overlapping/good, m/u = monitored/unmonitored
8
9   Read block of data points, find the Average
10 Call *Peak Detector* ($\underline{Threshold}$ + Average, $\underline{Width}$)
11 For each peak found {
12   Find Δt = time since last peak, A = peak amplitude
13   if (i = 0, 1, …, $\underline{N}$–2) { // peak that precedes last photobleaching beam
14   if ($\underline{Min}$ < Δt < $\underline{Max}$) {
15   i++; A[i] = A / A[0]; }
16   else {
17   Reset; } }
18   else if (i = $\underline{N}$–1) { // peak may be due to last photobleaching beam
19   if ($\underline{Min}$ < Δt < $\underline{Max}$) {
20   i++; A[i] = A / A[0]; S = false;
21   if ($\underline{LL}$[ ] < A[ ] < $\underline{UL}$[ ] and O = false) {
22   Calculate timing; Initiate selection; S = true; }}
23   else {
24   Reset; } }
25   else if (i = $\underline{N}$) { // peak that follows that from last photobleaching beam
26   if ($\underline{M}$ = 0) { // if no monitor beam is used
27   O2 = O; Reset;
28   if (O or O2) { if (S) { sou++; } else {nou++; } } else { if (S) { sgu++; } else {ngu++; } } }
29   else { // if a monitor beam is used, i.e., $\underline{M}$ = 1
30   if ((1–$\underline{\delta}$) $\underline{T_D}$ < Δt < (1+$\underline{\delta}$) $\underline{T_D}$) {
31   i ++; }
32   else {
33   O2 = O; Reset2;
34   if (O or O2) { if (S) { sou++; } else {nou++; } } else { if (S) { sgu++; } else {ngu++; } } } }
35   else if (i = $\underline{N}$+1) { // peak that follows that from monitor beam
36   O2 = O; Reset;
37   if (O or O2) { if (S) { som++; } else {nom++; } } else { if (S) { sgm++; } else {ngm++; } } } }
38 Go to line 9
39
40 Reset: i = 0; A[0] = A; if (Δt < $\underline{Max}$)   { O = true; } else {O = false; } Return;
41 Reset2: i = 0; A[0] = A; if (Δt < (1+$\underline{\delta}$) $\underline{T_D}$) { O = true; } else {O = false; } Return;

[a] Adjustable parameters are underlined; ++ means increment the counter by 1.

Software for real-time analysis of fluorescence peaks and control of cell sorter: Host PC program

Fig. S1 shows a screen shot of the Host PC program, captured during the execution of an experiment. The program, which runs on a PC that uses the Windows 7 operating system, receives the time and amplitude of each detected fluorescence peak over the network from the Target PC. It groups these peaks into bursts of peaks using the same algorithm that runs on the Target PC (as described above), but with its own (Host) values of adjustable parameters, to determine graphical representations of the passage of individual cells, and also the would-be sorting statistics displayed in the top right yellow box, i.e., those that would be obtained on the Target PC if that had used the same parameters. Thus at the start of an experiment, prior to turning on the 1064-nm "Laser Trap" for cell sorting, the parameters on the Host PC can be adjusted to optimize the grouping of peaks into bursts. These revised parameters can then be downloaded over the network to replace the parameters used by the Target PC, or otherwise discarded and replaced by values uploaded from the Target PC. The Target PC also collects its own (true) statistics, which are sent to the Host PC and displayed in the light blue region near top right.
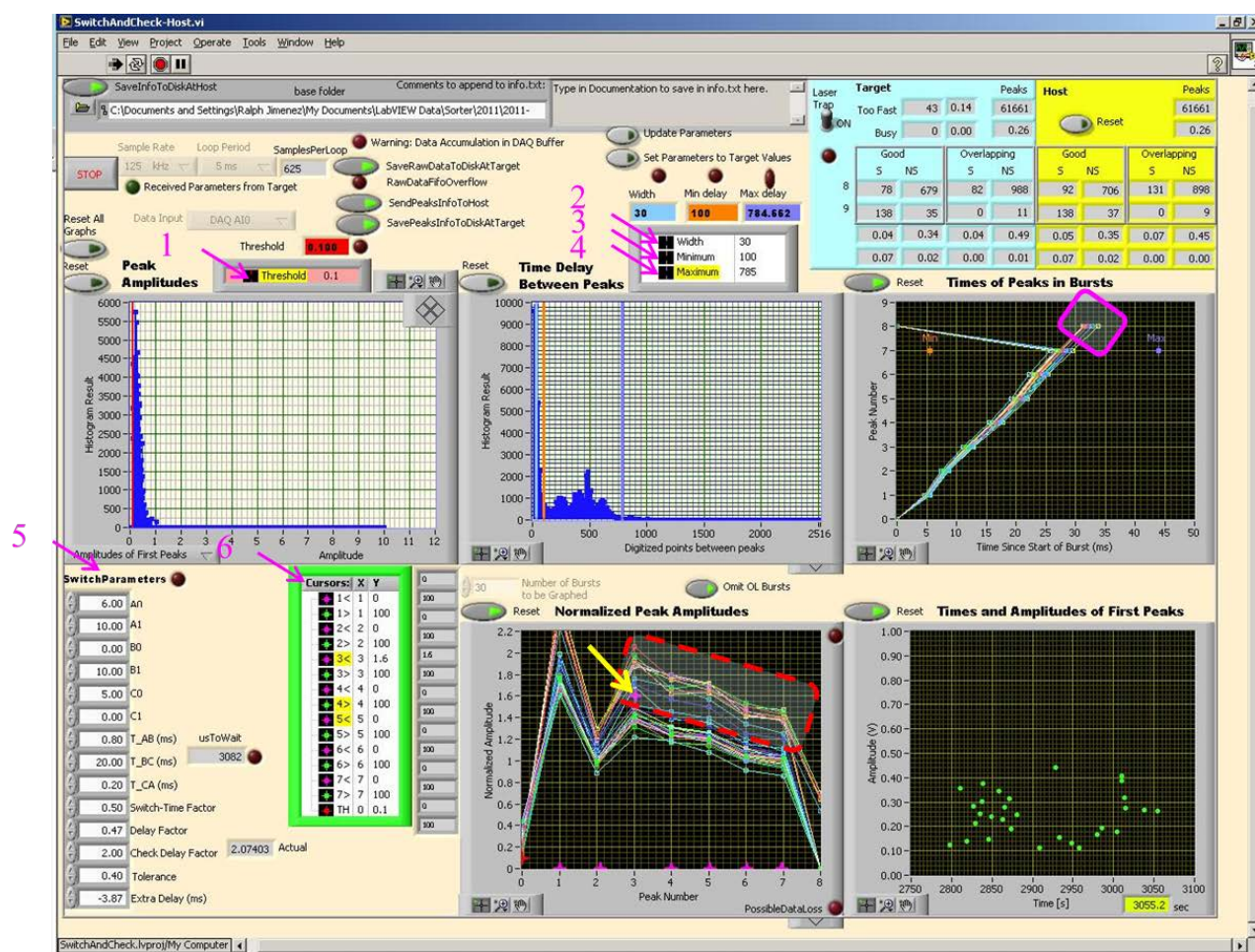

Fig. S1. Screen shot of Host PC interface program.

During this particular experiment, the 532-nm laser power was 0.98 W, with ~ 0.1 W in each of the 9 beams, while the 1064-nm laser power was 14 W. The flow speed was 8 mm/s (240 µm/30 ms) and the time for the 1064-nm spot to move from 2 to 3 in Fig. 4 was ~15 ms.

The adjustable parameters (indicated by pink numbered arrows) are: (1) Threshold, (2) Width, which together are used by the LabView point-by-point library routine *Peak Detector* to find the locations and amplitudes of peaks in the data stream; (3) Minimum (time delay), and (4) Maximum (time delay), which are used together with counting of the peaks in a burst to piece together the peaks into bursts of up to 8 peaks and to determine whether a burst is overlapping with a previous burst (designated as Overlapping) or not overlapping (designated as Good); (5) a set of Switch Parameters, which define the voltages at the 3 vertices of the piezo-mirror triangular trajectory(A0, A1, B0, B1, C0, C1), the time for motion along the legs of the trajectory, 12 (designated as T_AB), 23 (designated as T_BC and readjusted to be T_C), and 34 (designated as T_CA), the ratios B/A (Switch-Time Factor), C/A (Delay Factor), and F (D/A) (Check Delay Factor) needed to calculate the timings, the tolerance parameter δ (Tolerance) for designating a peak as due to a cell passing through the monitor beam, and an additional parameter (Extra Delay) to provide an empirically determined offset to T_B to account for slow-down of the flow near the junction and latency of the switch; (6) a set of values for peak amplitude ratios (listed within the green box), set by using the mouse to position cursors on the graph labelled **Normalized Peak Amplitudes**. These values select the photobleaching characteristics of cells that we wish to switch to the upper exit channel.

Note however, that the switch will only be attempted if the burst of fluorescence peaks from the cell is designated as Good (not Overlapping). The switch will also not be attempted if the calculated time to wait until the start of the switch cycle (shown as usToWait at lower left in Fig. S1) is negative, in which case the cell is counted as "Too Fast" (in blue box at top right Fig. S1); or if the piezo-mirror trajectory from the previous selection will not be completed in time, which is counted as "Busy" (in blue box at top right Fig. S1). After the peak of a burst as a cell passes the last photobleaching beam, whether the switch of the cell is selected (S) or not selected (NS), a peak that follows within a delay of $(1\pm\delta)T_D$ is categorized as due to that same cell passing the monitor beam and the burst is designated as having 9 peaks, but this may also be due to a new cell passing into beam 1. Thus the monitor beam provides an indication of a successful cell selection useful for setting up the instrument (and is visually indicated by extending the line in the graph of **Times of Peaks in Bursts**, as highlighted within the pink diamond shape in Fig. S1), but as discussed in the main body of the paper, it over-counts the cells that pass into the sort channel (the bursts that have 9 peaks), particularly those cells that were not selected. While the success of a sort must ultimately be determined by further analysis of the sorted population of cells (as is reported in the section **Cell selection based on irreversible photobleaching** near the end of the body of the paper), the monitor beam provides data from which a lower limit of the purity of the sort can be determined. For the data displayed in Fig. S1, this is: Relative purity > 9GS/(9GS+9GNS) = 138/(138+35) = 0.8.

Calibration measurements

The following four figures are referenced in the body of the paper in the section **Results and discussion**.
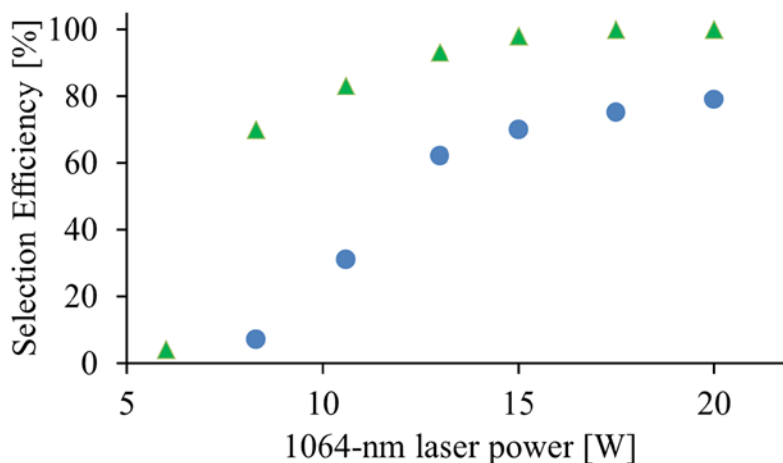

Fig. S2 Cell selection efficiency vs. 1064-nm laser power for: (i) cell suspension medium (lower curve,●), or (ii) buffer without Optiprep (upper curve,▲), in the side channels used for hydrodynamic focusing.
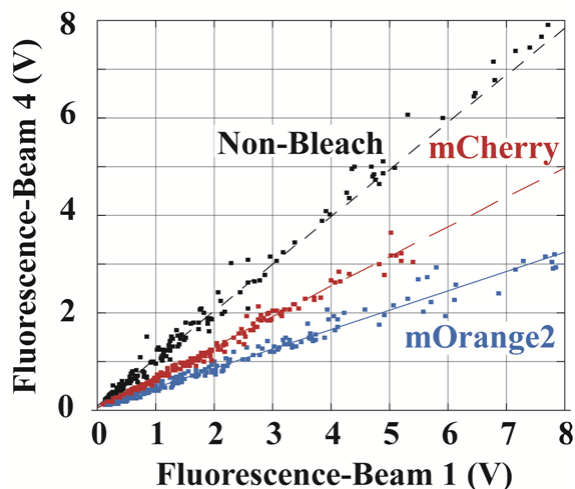

Fig. S3 The fluorescence signal voltage from beam 4 vs. that from beam 1. The non-bleach assay is obtained using fluorescent beads labelled with small molecule dyes that demonstrate negligible photobleaching in the cytometer (Invitrogen, F-8858 fluospheres, 4 μm, 580/605). The mCherry and mOrange2 curves are obtained from a mixture of HeLa-S cells expressing either mCherry or mOrange2. Note that mCherry is more photostable than mOrange2 under these excitation conditions.

From the data in Fig. S3 above, the ratios of the signal voltages (beam 4/beam 1) are $R_i \sim 0.63$ or 0.40, where i is for cells with mCherry or mOrange2. These ratios may be used to estimate lower limits for the photodestruction quantum yields Φ_i, which are found to be $\Phi_{mCherry} = 8.7 \times 10^{-6}$ and $\Phi_{mOrange2} = 1.5 \times 10^{-5}$. The ratio of the signal voltages for mCherry is 1.58 times that of mOrange2, whereas the estimated photodestruction quantum yield is 1.75 times smaller.

The estimates are found as follows: The ratios are $R_i = \exp(-\Phi_i N_i)$, where N_i is the mean number of excitations a fluorescent molecule would undergo (if not photo-destroyed) as it transits through 3 beams (from after beam 1 to after beam 4). As each beam has a line-focused Gaussian intensity profile given by

$$I(x, y) = \frac{2P}{\pi \omega_x \omega_y} \exp\left[\frac{-2x^2}{\omega_x^2}\right] \exp\left[\frac{-2y^2}{\omega_y^2}\right],$$

where $P = 0.09$ W is the power of each beam, and $\omega_x \sim 3 \times 10^{-4}$ cm, $\omega_y \sim 6.7 \times 10^{-3}$ cm are the radii across and along the line, we may estimate

$$N_i = \frac{3\sigma_i}{E_\gamma} \int_{-\infty}^{\infty} I(vt, 0)\, dt = \frac{3\sigma_i}{E_\gamma} \int_{-\infty}^{\infty} \frac{2P}{\pi \omega_x \omega_y} \exp\left[\frac{-2v^2 t^2}{\omega_x^2}\right] dt = \frac{3\sigma_i}{E_\gamma} \frac{2P}{\pi \omega_x \omega_y} \sqrt{2\pi} \frac{\omega_x}{2v},$$

where σ_i is the absorption cross-section, $E_\gamma = 3.74 \times 10^{-19}$ J is the energy of the 532-nm photons, and $v = 0.6$ cm/s is the flow speed. This gives

$$\Phi_i = \frac{-\ln(R_i) \sqrt{2\pi} E_\gamma \omega_y v}{6\sigma_i P},$$

or using $\sigma_i = 3.82 \times 10^{-21} \varepsilon_i$, where σ_i is in units of cm^2 and ε_i is the molar extinction coefficient expressed in units of L mol^{-1} cm^{-1}, we have

$$\Phi_i = \frac{-\ln(R_i) 40.9 \omega_y v}{\varepsilon_i P},$$

where $\varepsilon_{mCherry} = 97{,}000$ M^{-1} cm^{-1} and $\varepsilon_{mOrange2} = 110{,}000$ M^{-1} cm^{-1}, as given in [5]. The above estimates for Φ_i are lower limits as they do not account for a decrease in the number of excitations N_i due to refraction losses or saturation effects from reversible dark state conversion.
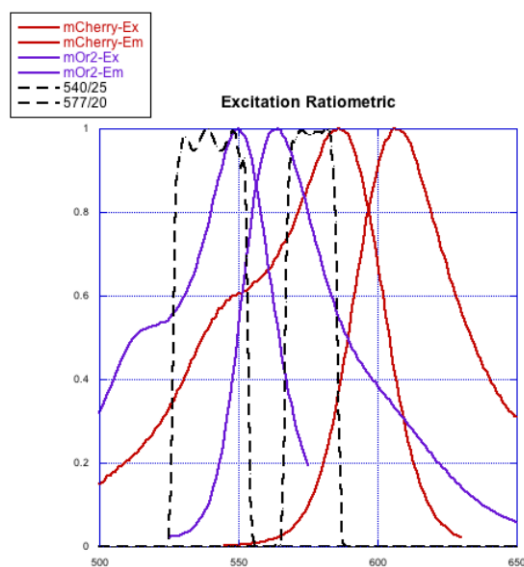

Fig. S4 The fluorescence excitation (left) and emission (right) spectra of mOrange2 (solid purple curves) and mCherry (solid red curves) and the transmission (dashed black curves) of the two fluorescence excitation filters, 527–553 nm (left) and 567–587 nm (right). The identity of imaged cells is determined from the ratio of the fluorescence signals obtained from each of the excitation bands.
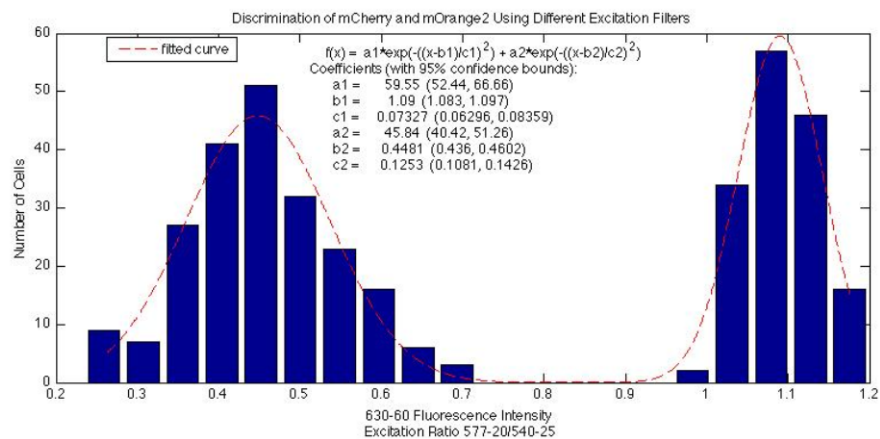
Discrimination of mCherry and mOrange2 Using Different Excitation Filters

$f(x) = a1^\ast\exp(-((x-b1)/c1)^2) + a2^\ast\exp(-((x-b2)/c2)^2)$
Coefficients (with 95% confidence bounds):
a1 =   59.55 (52.44, 66.66)
b1 =   1.09 (1.083, 1.097)
c1 =   0.07327 (0.06296, 0.08359)
a2 =   45.84 (40.42, 51.26)
b2 =   0.4481 (0.436, 0.4602)
c2 =   0.1253 (0.1081, 0.1426)

630-60 Fluorescence Intensity
Excitation Ratio 577-20/540-25

Fig. S5 Histogram of the ratiometric excitation (i.e., fluorescence for 567–587 nm excitation / fluorescence for 527–553 nm excitation) showing clear resolution of mCherry cells (right peak) from mOrange2 cells (left peak).